



HHS Public Access

Author manuscript

Nat Struct Mol Biol. Author manuscript; available in PMC 2012 January 01.

Published in final edited form as:

Nat Struct Mol Biol. ; 18(7): 805–812. doi:10.1038/nsmb.2061.

Synaptotagmin-1 may be a distance regulator acting upstream of SNARE nucleation

Geert van den Bogaart¹, Shashi Thutupalli², Jelger H. Risselada³, Karsten Meyenberg⁴, Matthew Holt¹, Dietmar Riedel⁵, Ulf Diederichsen⁴, Stephan Herminghaus², Helmut Grubmüller³, and Reinhard Jahn¹

¹Department of Neurobiology, Max Planck Institute for Biophysical Chemistry, Am Faßberg 11, 37077, Göttingen, Germany

²Department of Dynamics of Complex Fluids, Max Planck Institute for Dynamics and Self-Organization, Bunsenstr. 10, 37073, Göttingen, Germany

³Department of Theoretical and Computational Biophysics, Max Planck Institute for Biophysical Chemistry, Am Faßberg 11, 37077, Göttingen, Germany

⁴Institute for Organic and Biomolecular Chemistry, Georg-August-University, Tammannstraße 2, 37077, Göttingen, Germany

⁵Facility for Electron Microscopy, Max Planck Institute for Biophysical Chemistry, Am Faßberg 11, 37077, Göttingen, Germany

Abstract

Synaptotagmin-1 triggers Ca²⁺-sensitive, rapid neurotransmitter release by promoting the interaction of SNARE proteins between the synaptic vesicles and the plasma membrane. How synaptotagmin-1 promotes this interaction is controversial, and the massive increase in membrane fusion efficiency of Ca²⁺-synaptotagmin-1 has not been reproduced *in vitro*. However, previous experiments have been performed at relatively high salt concentrations, screening potentially important electrostatic interactions. Using functional reconstitution in liposomes, we show here that at low ionic strength SNARE-mediated membrane fusion becomes strictly dependent on both Ca²⁺ and synaptotagmin-1. Under these conditions, synaptotagmin-1 functions as a distance regulator: tethering the liposomes too far for SNARE nucleation in the absence of Ca²⁺, but brings the liposomes close enough for membrane fusion in the presence of Ca²⁺. These results may explain how the relatively weak electrostatic interactions of synaptotagmin-1 with membranes substantially accelerate fusion.

Users may view, print, copy, download and text and data- mine the content in such documents, for the purposes of academic research, subject always to the full Conditions of use: http://www.nature.com/authors/editorial_policies/license.html#terms

Correspondence should be addressed to R.J. (R.Jahn@gwdg.de).

Author contributions

S.T. and S.H. performed the flow cytometry experiments. J.H.R. and H.G. performed the M.D. simulations. M.G.H purified the synaptic vesicles. Thermophoresis data is from K.M. and U.D. D.R. performed the EM. G.v.d.B performed all other experiments. G.v.d.B. and R.J. designed the study and wrote the paper. All authors discussed the results and commented on the manuscript.

Presynaptic nerve terminals convert electrical signals into chemical signals that target other neurons or somatic cells. The conversion is mediated by a depolarisation of the plasma membrane, which causes an influx of Ca^{2+} through voltage activated Ca^{2+} -channels. The increase of the local cytoplasmic Ca^{2+} concentration triggers the submillisecond fusion of synaptic vesicles with the plasma membrane. Membrane fusion is mediated by the assembly of SNARE proteins including the R-SNARE synaptobrevin-2 (also known as VAMP2) on the synaptic vesicle and the Q-SNAREs syntaxin-1A and SNAP-25 on the plasma membrane^{1,2}. SNARE assembly involves the conserved, membrane-adjacent SNARE motifs, proceeds from the N-terminus towards the C-terminal membrane anchors, and results in formation of a tight coil-coil structure which pulls the membranes together and overcomes the energy barrier of membrane fusion.

The synaptic vesicle protein synaptotagmin-1 functions as a major Ca^{2+} -sensor for neuronal exocytosis^{3,4}. The 65 kDa protein contains a single transmembrane domain followed by a large cytoplasmic domain consisting of a 61 residue unstructured linker and tandem C2-type domains. These C2-domains, called the C2A- and C2B-domain, bind 2 and 3 Ca^{2+} ions respectively with low affinity ($60 \mu\text{M} - 1 \text{mM}$)^{5,6} and interact with both anionic membranes and SNARE proteins. Synaptotagmin-1 binds to anionic lipids both in the absence of Ca^{2+} via a so-called polybasic patch consisting of four lysines located on the C2B-domain⁷⁻⁹ and in the presence of Ca^{2+} via its Ca^{2+} -binding sites^{5,8-13}. Anionic lipids such as phosphoserine (PS) and phosphatidylinositol 4,5-biphosphate ($\text{Pi}(4,5)\text{P}_2$) complete the Ca^{2+} -binding sites of the C2-domains and thereby increase the affinity of synaptotagmin-1 for Ca^{2+} -binding^{5,7,8,14}. Ca^{2+} -synaptotagmin-1 locally increases membrane curvature, suggesting that synaptotagmin-1 might act by increasing the membrane tension at the sites of fusion^{15,16}. Synaptotagmin-1 also binds directly to SNAP-25, syntaxin-1A, and the binary and ternary SNARE complexes^{3,17-19}. All together, a model is emerging where synaptotagmin-1 structurally changes both the SNARE complex and the membranes in a Ca^{2+} -dependent manner, thereby levering the protein and/or bending the membrane which induces membrane fusion^{3,9,11,15-22}. Importantly, in these models, synaptotagmin-1 acts downstream of SNARE nucleation, *i.e.* at a fusion-arrested state where the membranes are tethered by a *trans* SNARE-complex in which at least part of the cytoplasmic SNARE-domains, but not the C-terminal transmembrane helices, are already coiled up.

A large number of studies aimed to reconstitute Ca^{2+} -synaptotagmin-1 triggered membrane fusion *in vitro* using SNARE-containing artificial membranes, either by adding the soluble cytoplasmic C2-domains (C2AB fragment; residues 97–421) or by inserting full-length membrane-anchored synaptotagmin-1. A major limitation in these studies is that SNAREs alone are sufficient to induce lipid mixing of liposomes²³. Indeed, membrane fusion is relatively efficient when artificial membranes containing even a single copy²⁴ of synaptobrevin-2 and a combination of syntaxin-1A and SNAP-25 are mixed. The addition of the soluble C2AB fragment makes membrane fusion somewhat Ca^{2+} -sensitive and results in an increase of fusion efficiency between $100 \mu\text{M}$ and 10mM Ca^{2+} (mainly lipid mixing)^{3,10,11,15,16,20,21,25-29}. However, in these studies, membrane fusion still proceeds in the absence of the C2AB fragment and the increase in fusion efficiency is usually less than 10-fold compared to the over 18,000-fold increase *in vivo*³⁰. Recently, it was reported that

lipid mixing in the presence of membrane-anchored synaptotagmin-1 was increased about 3–5-fold at 10 μM Ca^{2+} but decreased again at higher Ca^{2+} concentrations²⁷. This Ca^{2+} -dependency was strongly influenced by the lipid composition of both liposome populations: increasing the fraction of anionic lipids in the Q-SNARE or R-SNARE membranes resulted in higher or lower Ca^{2+} -sensitivities, respectively.

There is general consensus that the interactions of synaptotagmin-1 with membranes and SNAREs are predominantly of an electrostatic nature. Indeed, binding of synaptotagmin-1 both to anionic lipid membranes^{5,7} and to SNARE molecules^{18,19,22} is heavily influenced by the ionic strength of the solution. Thus, it is surprising that the influence of ionic interactions on membrane fusion in the presence of synaptotagmin-1 has not been investigated: All aforementioned *in vitro* synaptotagmin-1 membrane fusion studies were performed at relatively high, physiological ionic strength and typically 100 to 150 mM KCl or NaCl. However, at these high salt concentrations the binding of synaptotagmin-1 to SNAREs and anionic membranes is strongly reduced or even absent^{5,7,18,19,22}. We thus set out to answer the question of how ionic strength influences synaptotagmin-1 action.

Results

Membrane fusion is blocked at low ionic strength

SNARE mediated liposome fusion is typically studied at physiological ionic strength, with NaCl or KCl concentrations of 100–150 mM^{3,5,10,11,15,16,20,21,25–29} where the Debye charge screening length is only ~ 7 Å. Molecules need to be within a few times this distance to interact. We studied SNARE-mediated fusion at low ionic strength by employing a FRET-based lipid mixing assay (without synaptotagmin-1; Fig. 1a). The R-SNARE population of liposomes contained a 1:1,000 molar protein-to-lipid ratio of recombinant synaptobrevin-2 and was labeled with the fluorescent lipid analog Oregon green-phosphatidylethanolamine (OG-PE; donor fluorophore). The Q-SNARE population of liposomes contained 1:2,000 of a complex consisting of two copies of recombinant syntaxin-1A (lacking its inhibitory N-terminal Habc-domain^{31–33}; residues 183–288) and a single SNAP-25 (2:1-complex)²⁵. Those liposomes were labeled with DiD (acceptor fluorophore). As already shown in numerous studies^{3,10,11,15–16,20,21,23–29,32–34,35–38}, robust, SNARE specific lipid mixing was observed at normal ionic strength (20 mM K-Hepes pH 7.4, 150 mM KCl; Fig. 1a). Surprisingly however, lipid mixing was almost completely blocked at low ionic strength (20 mM K-Hepes pH 7.4, 5 mM KCl, 300 mM sucrose) where the Debye screening length was ~ 25 Å. Lipid mixing at low ionic strength was also blocked with 1:8,000 molar protein-to-lipid ratio of the binary Q-SNARE complex stabilized with a fragment of synaptobrevin-2 (residues 49–96; Fig. 1b). This stabilized complex ensures that all Q-SNAREs are available for fusion and displays a dramatically enhanced fusion efficiency compared to native Q-SNAREs³⁴. These results indicate that the absence of lipid mixing at low ionic strength was not due to unavailability of the binary Q-SNARE complex. Reversing the fluorescent labels or increasing the SNARE density up to 1:500 showed similar results.

We were unable to incorporate SNARE proteins in the liposomes at salt concentrations below 150 mM and had to reduce the ionic strength by diluting the liposomes afterward. Sucrose was added to preserve the osmolarity at ~ 340 mOsm. Membrane fusion was still

blocked at low ionic strength when the sucrose was omitted, but the liposomes looked osmotically deformed by negative-staining electron microscopy (EM; Fig. 1b) and the liposomes became leaky at osmotic differences above 100 mOsm (Supp. Fig. 1a). The presence of sucrose increased the viscosity 33% and this decreases the diffusion of both soluble and membrane associated³⁹ molecules. Diffusion limited reactions are slowed accordingly⁴⁰.

The liposomes contained ~10% anionic lipids, and we speculated that the electrostatic repulsion might be too high for SNARE-mediated membrane fusion at low ionic strength. To validate this hypothesis, we performed experiments with liposomes composed of pure zwitterionic phosphatidylcholine (PC; Fig. 1c–d). Indeed, without PS, lipid mixing at low ionic strength still occurred, albeit somewhat slower than at normal ionic strength because of the sucrose (increased viscosity). In contrast, lipid mixing was completely blocked with 10% PS at low but not at normal ionic strength. Thus, the electrostatic repulsion at low ionic strength increases the energy barrier of membrane fusion. We then tested whether SNARE nucleation could still occur under these conditions.

SNARE complex formation was directly followed by FRET with liposomes containing a 1:8,000 protein-to-lipid ratio of the stabilized Q-SNARE-complex with syntaxin-1A labeled with Alexa fluor 488 (S225C; donor fluorophore)^{32,35}. Mixing these liposomes with 100 nM of the soluble synaptobrevin-2_{1–96} fragment labeled with Texas red (S61C; acceptor fluorophore)³⁵ resulted in fast complex formation independent of ionic strength (Fig. 1e). Accordingly, mixing liposomes containing full-length synaptobrevin-2 with a soluble Q-SNARE complex (SNAP-25, syntaxin-1A_{183–262} and synaptobrevin-2_{49–86}) also resulted in complex formation, albeit somewhat slower. This decrease is probably due to increased electrostatic repulsion at low ionic strength (the Q-SNARE complex has an acidic surface). In contrast to the soluble SNAREs, SNARE complex formation was only observed at normal but not at low ionic strength when liposomes bearing membrane-anchored Q- and R-SNAREs were used (Fig. 1f), thus paralleling lipid mixing. These FRET data were in perfect agreement with the dissociation of the synaptobrevin-2_{49–96} fragment from the stabilized acceptor complex (Supp. Fig. 1b–c). Thus, we conclude that although SNARE zippering can occur at low ionic strength, the high electrostatic repulsion between the liposomes blocks not only lipid mixing but also SNARE nucleation.

Ca²⁺-synaptotagmin-1 action at low ionic strength

Next, we studied whether synaptotagmin-1 rescues membrane fusion at low ionic strength. We reconstituted recombinant full-length synaptotagmin-1 at a protein-to-lipid ratio of 1:4,000 in the R-SNARE liposomes. At normal ionic strength, synaptotagmin-1 somewhat increased the lipid mixing kinetics independent of Ca²⁺ (Fig. 2a–b), as reported previously^{25,29}. In contrast, lipid mixing was almost completely blocked at low ionic strength and 1 mM Ca²⁺ now dramatically increased lipid mixing. This lipid mixing was strictly dependent on both synaptotagmin-1 and the SNAREs. Under those low ionic strength conditions, the C2-domains of synaptotagmin-1 are correctly folded and specifically bind Ca²⁺ (Supp. Fig. 2). Experiments where Ca²⁺ was mixed by controlled flow focusing in a microfluidics flow chamber⁴¹ showed that fusion could be readily triggered with Ca²⁺

(Fig. 2c–e). Compared to cuvette-based experiments, flow cytometry allows for relatively fast and well controlled mixing. Moreover, under our conditions, the synaptotagmin-1 mediated membrane fusion efficiency correlated with the Ca^{2+} concentration in a dose dependent manner from 10 μM up to 1 mM Ca^{2+} and Mg^{2+} had only little effect (Fig. 2f–g). This Ca^{2+} sensitivity depends on precise protein densities and compositions of the membranes and buffer²⁷.

At normal ionic strength, purified synaptic vesicles from rat brain fuse independent of Ca^{2+} (ref. 37). However, as these membranes contain about 15% anionic lipids⁴², it seemed possible that (similar to the liposomes) membrane fusion of synaptic vesicles becomes Ca^{2+} -sensitive at low ionic strength. To test this hypothesis, we fused synaptic vesicles with Q-SNARE liposomes containing both donor and acceptor fluorophores. In this case, membrane fusion dilutes the fluorescent lipid analogs with the vesicle membranes, resulting in a loss of FRET and a decrease of acceptor fluorescence. Indeed, at low ionic strength, lipid mixing was largely Ca^{2+} -dependent (Fig. 2h). Thus, at low ionic strength Ca^{2+} -synaptotagmin-1 triggers lipid mixing not only of liposomes, but also of native synaptic vesicles.

Because lipid mixing does not distinguish between hemifusion and full membrane fusion, it is conceivable that the membrane fusion did not progress beyond the hemifusion state. To resolve this issue, we employed a content mixing assay where liposomes with encapsulated calcein at self quenching concentrations were fused with empty (calcein-free) liposomes²⁴. Content mixing results in calcein dequenching. Indeed, a SNARE and Ca^{2+} -synaptotagmin-1 specific increase in fluorescence was observed (Fig. 3a). This content mixing was not caused by leakage of the calcein from the liposomes, as leakage was only 4–5% of total calcein (Supp. Fig. 3a). In addition, FRET and fluorescence anisotropy measurements indicated that there was no SNARE nucleation without Ca^{2+} (Fig. 1e–f, 3b–e). In the absence of synaptotagmin-1, some residual SNARE complex formation was observed (Fig. 1e, 3c), which we attribute to charge-shielding by the bivalent Ca^{2+} cations, which allows for a low degree of SNARE interaction and membrane fusion. SNARE complex formation was inhibited by synaptobrevin-2_{1–96} even when added after the mixing of the R- and Q-SNARE liposomes, and regardless of whether wild-type synaptotagmin-1 was used, or a mutant in which two lysines of the polybasic patch are converted to alanines (K325A K326A; KAKA-mutant⁷; Fig. 3d–e). This indicates that no substantial SNARE nucleation occurred without Ca^{2+} .

Disrupting Ca^{2+} -binding of the C2A-domain (D178A D230A D232A) reduced both the lipid-mixing and SNARE-complex formation substantially (Fig. 3f–g). In contrast, the corresponding C2B-mutant (D309A D363A D365A) had little effect on the membrane fusion efficiency. This has been reported before^{11,16,25}, but contradicts *in vivo* data where disruption of Ca^{2+} -binding to the C2B-domain impaired release much more severely than C2A disruption⁴³. This discrepancy may be because –unlike in the synapse– both fusion partners are small liposomes, which bypasses the requirement for membrane bending by the C2B-domain^{15,16}. To evaluate whether membrane curvature influences the ability of the C2B-domain to stimulate membrane fusion at low ionic strength, we performed experiments with 10–20 μm giant unilamellar vesicles (GUVs; Fig. 3h). These membranes are much less curved than the small 36 nm-sized²⁴ liposomes used elsewhere in this study. Fusing the

GUVs with small synaptotagmin-1–synaptobrevin-2 liposomes showed that fusion was abolished when Ca^{2+} -binding was disrupted to the C2B-mutant, similar to normal ionic strength¹⁶. Importantly, fusion of the C2B-mutant could be rescued by disruption of the GUVs by sonication (Supp. Fig. 3b). All together, we conclude that at low ionic strength Ca^{2+} -synaptotagmin-1 triggers SNARE-mediated membrane fusion and both C2-domains are required.

Synaptotagmin-1 acts as a distance regulator

Synaptotagmin-1 binds to anionic lipids both with and without Ca^{2+} and this binding leads to membrane clustering^{5,7–13,25}. Indeed, negative-staining EM showed strong instantaneous clustering of the liposomes when synaptotagmin-1 liposomes were mixed with empty liposomes (no SNAREs; Supp. Fig. 4a). This clustering was $\text{Pi}(4,5)\text{P}_2$ and synaptotagmin-1 specific and was reduced when the KAKA mutant of synaptotagmin-1 was used (Supp. Fig. 4b), similar to normal ionic strength⁹. Identical results were obtained when the SNAREs were present. The clustering of liposomes by synaptotagmin-1 was confirmed with dynamic light scattering (DLS) experiments (Fig. 4a, Supp. Fig. 4c). In addition, we developed a microscale thermophoresis⁴⁴ assay to assess liposome clustering without Ca^{2+} (Fig. 4b–c). For this, DiD-labeled liposomes were inserted in a capillary that was heated $\sim 5^\circ\text{C}$ locally with a focused infrared laser. Because of the Soret-effect⁴⁵, these liposomes thermodiffused away from the heated spot, hence creating a local drop in the concentration and fluorescence intensity (= positive thermophoresis). The extent of this depletion depends on the surface properties of the liposomes (solvation entropy). Contrary to the DiD-liposomes, liposomes labeled with sufficient (>5 mol%) OG-PE thermodiffuse towards the heated spot and are locally enriched (= negative thermophoresis). Thus, DiD-liposomes are separated from OG-PE-liposomes by the heating laser, unless they are tethered by synaptotagmin-1 in which case they co-segregate resulting in intermediate thermophoresis. This tethering was dependent on $\text{Pi}(4,5)\text{P}_2$ and was reduced when the KAKA mutant of synaptotagmin-1 was used, all in agreement with the DLS and EM data. Density gradient flotation experiments with various mutants of the soluble C2AB-domain showed that without Ca^{2+} the polybasic lysine patch of synaptotagmin-1 bound to membranes, whereas binding with Ca^{2+} occurred primarily via the Ca^{2+} -binding sites (Supp. Fig. 4d)^{7,9}.

In the EM images, synaptotagmin-1 tethered the liposomes at very narrow distances even without Ca^{2+} ('squeezed together'; Supp. Fig. 2a; Fig. 4d). Regardless of this tight liposome association, SNARE nucleation did not occur under those conditions (Fig. 3b–e) suggesting that the vesicles are still separated by a distance too far for *trans* SNARE interactions (Fig. 4e). However, negative-staining EM involves fixation and drying and is thus unsuitable for assessing membrane distances. We could not perform cryo-EM, because of the presence of sucrose to compensate for the osmolarity. Therefore, we used the FRET approach of Yoon *et al.*⁴⁶ (Fig. 4f–g, Supp. Fig. 4e), based on the $\sim 5\%$ FRET resulting from clustering of DiI with DiD labeled liposomes at distances below ~ 5 nm. In the presence of synaptotagmin-1 (no SNAREs), no FRET signal was detectable although the vesicles were clustered (Fig. 4a–c, Supp. Fig. 4a–d). Accordingly, Ca^{2+} induced FRET of both the wild-type and the KAKA mutant and this increased substantially when 1% $\text{Pi}(4,5)\text{P}_2$ was present. Disrupting Ca^{2+} -binding to the C2A- or C2B-domain largely impaired this FRET signal. The observed FRET

was caused by close membrane proximity rather than by residual lipid mixing, because the FRET signal was reversed by addition of 1 mM EDTA. Lastly, dynamic light scattering experiments with the C2AB fragment (Fig. 4h; Supp. Fig. 4f) showed that this fragment was sufficient for liposome clustering in the presence of Ca^{2+} , similar to normal ionic strength⁹.

Together, we conclude that without Ca^{2+} the polybasic patch of synaptotagmin-1 tethers the liposomes too far for SNARE nucleation. Ca^{2+} binds to the C2AB-domain, which functions as a ‘charge bridge’ bringing the membranes close enough for SNARE nucleation. A comparison of wild-type synaptotagmin-1 and the KAKA mutant (with reduced membrane tethering) indicates that this tethering can accelerate lipid mixing at low, rate-limiting concentrations of liposomes (Fig. 5a), but not at higher concentrations (Supp. Fig. 5a), in agreement with the weak phenotype of the KAKA mutant^{7,47}. A specific interaction between synaptotagmin-1 and the neuronal SNAREs does not seem required, because the SNAREs of constitutive exocytosis (SNAP-23 and syntaxin-4 without Habc-domain; residues 191–298) can also mediate Ca^{2+} -synaptotagmin-1-triggered membrane fusion (Fig. 5b). These findings are not surprising since SNARE interaction of Ca^{2+} -synaptotagmin-1 is not required to bring two membranes in close proximity (Fig. 4)⁹. However, this contradicts earlier data on the C2AB fragment^{11,25}, likely because: (i) These studies were performed with much higher SNARE densities and at normal ionic strength where synaptotagmin-1–SNARE interactions may help tethering of the liposomes²⁵ and/or may modulate the SNAREs^{3,9,11,15,16,18–22}. (ii) We cannot exclude that synaptotagmin-1 interacts with SNAP-23–syntaxin-4 at low ionic strength. Lastly, lipid mixing experiments showed that liposome tethering at close distance by the Ca^{2+} -bound C2AB fragment is sufficient to trigger membrane fusion (Supp. Fig. 5b), similar to normal ionic strength^{3,10,11,15,16,20,25–29}.

We estimated how far synaptotagmin-1 could tether two membranes in various conformations with coarse-grain molecular dynamics simulations^{48,49}. The C2AB-domain was simulated based on the crystal structure (PDB 1DQV)⁵⁰. Each individual C2-domain was conformationally fixed, but had full translational and rotational mobility and was connected by a flexible linker (residues 266–273), as supported by NMR data^{9,18}. We then pulled pair-wise on the Ca^{2+} -binding patches, the polybasic patch and the N-terminus (Fig. 6a). The distances between those sites reflect the maximum length that synaptotagmin-1 can connect two membranes and are determined by the interconnecting linker and the surface interactions between the C2-domains. These distances are overestimates, because membrane insertion and bending are not accounted for. The distance from the polybasic patch to the transmembrane helix is ~28 nm (including the ~23 nm linker). However, the distance synaptotagmin-1 tethers liposomes without Ca^{2+} is likely shorter since the Debye length is only ~25 Å, but higher than the ~5 nm⁴⁶ from the FRET experiments (Fig. 4f–g). The maximum distances the Ca^{2+} -bound C2AB-domain could span two membranes is ~2–7.5 nm, close to the 4 nm from cryo-EM⁹. These distances would explain why decreasing the ionic strength and increasing the Debye length from ~7 to 25 Å has such a dramatic effect on membrane fusion. Thus, at low ionic strength, Ca^{2+} changes the membrane distance from 5–28 nm to below that required for SNARE complex formation (8 nm at normal ionic strength³⁶) such that membrane fusion can occur.

Discussion

At low ionic strength synaptotagmin-1 can regulate membrane fusion upstream of SNARE nucleation by acting as a distance regulator. In the absence of Ca^{2+} , the polybasic patch on the C2B-domain tethers the liposomes, but the electrostatic repulsion keeps them too far apart for SNARE complex formation to occur (Fig. 6b; step A). The linker connecting the C2AB-domain to the vesicle membrane is 61 residues long (residues 81–142) which means it can extend to maximum ~ 23 nm (0.38 nm residue⁻¹); a distance longer than the $\sim 2 \times 25$ Å electrical double layers separating the membranes. Ca^{2+} acts as a charge bridge, and the Ca^{2+} -bound C2AB-domain docks the vesicles at a closer distance where SNARE complex formation and membrane fusion can occur (step B). Similar models where synaptotagmin-1 functions as a membrane tethering factor have been proposed previously^{9,21,51} and we now present direct evidence that, at least at low ionic strength, such a mechanism can indeed trigger membrane fusion.

We needed low ionic strength to assure that the membrane repulsion was large enough to prevent SNARE nucleation. Although this condition does not reflect physiological conditions, an intermediate state was isolated at which vesicles can be tethered (*e.g.* by synaptotagmin-1) but the distance between the membranes was too high for synaptotagmin-1 independent membrane fusion and synaptotagmin-1 mediated reworking of the SNAREs and the membranes^{3,9,11,15–22}. Ca^{2+} binding to synaptotagmin-1 reduced the distance between the docked membranes, bringing them close enough for SNARE nucleation and subsequent fusion. Although specific increases in membrane fusion efficiency have been reported previously for both the C2AB fragment^{3,10,11,15,16,20,21,25–29} and full-length synaptotagmin-1²⁷, this increase is larger in our case because ‘background’ fusion (*i.e.* in the absence of synaptotagmin-1 or Ca^{2+}) is essentially blocked by keeping the membranes apart at low ionic strength. Thus, our finding adds a new facet to the still controversially discussed mechanism of synaptotagmin-1 action in exocytosis and may help in interpreting many of the often controversial data on synaptotagmin-1 mediated fusion of liposomes^{3,10,11,15,16,20,25–29}. The question is how this mechanism is integrated in the molecular steps governing vesicle docking and fusion in the synapse. In our opinion, two alternative scenarios are possible: one ‘mainstream’ scenario in which synaptotagmin-1 acts downstream of SNARE nucleation (which does not preclude an additional earlier role in docking⁵²), and an alternative scenario according to which SNAREs are not in *trans*-contact with each other before synaptotagmin-1 receives the Ca^{2+} signal.

In the first case, docked and primed synaptic vesicles are characterized by the SNAREs being partially zippered in *trans* as depicted in virtually all current models^{1–4}. Further zippering is prevented by an energy barrier that may involve membrane straining and/or inhibitory proteins such as complexins. Indeed, mutants interfering with either N-terminal or C-terminal SNARE zippering had profoundly different effects on exocytosis in chromaffin cells, which can be best explained by kinetically separate states (*i.e.* docking and fusion)⁵³. Accordingly, synaptotagmins’ ability to pull membranes a bit closer together may contribute to the overcoming of the energy barrier by relieving strain, in addition to an increase in local curvature and/or an activation/disinhibition of C-terminal SNARE zippering^{3,9,11,15–22}.

In the second case, Ca²⁺-synaptotagmin-1 would trigger membrane fusion by rapidly decreasing the distance between the vesicles and the plasma membrane, thus allowing SNARE nucleation to occur (as proposed previously⁵¹). Thus, SNARE nucleation takes place after Ca²⁺-influx similar to our findings (Fig. 6b). Indeed, it is still not resolved whether docked vesicles have their SNARE complexes arrested in a partially assembled complex⁵³. There are good reasons for challenging the view that a metastable *trans* SNARE-complex represents an energy minimum along the fusion pathway. Firstly, knocking out synaptobrevin-2^{54,55} or cleaving it with tetanus neurotoxin⁵⁶ does not affect vesicle docking, in opposition with a requirement of SNARE nucleation for docking. Secondly, it is difficult to understand how a strained and partially zippered SNARE complex can be arrested, especially considering that only 1–3 SNARE complexes are required for membrane fusion^{24,57}. At least *in vitro*, even the synaptobrevin-2_{49–96} fragment (which binds with nM affinity to the Q-SNAREs) cannot block membrane fusion³⁴. Whereas both candidates for such a clamping role, synaptotagmin-1²⁶ and complexin^{20,22} can reduce membrane fusion, they bind with much lower affinity to the Q-SNARE complex than synaptobrevin-2_{49–96}. While effective energies may be different at the fusion site, there is so far no strong and direct evidence for any of these proteins slowing or even preventing SNARE assembly.

In summary, our data show that in a simple reconstituted system, key elements of synaptic transmission can be mimicked if SNARE nucleation is prevented by keeping the membranes apart before Ca²⁺-triggering. Under these conditions, no fusion occurs although SNAREs are fully active, but fusion is ‘unleashed’ as soon as the membranes are pulled a bit closer by Ca²⁺-dependent membrane binding of the C2-domains (Fig. 6b). While we needed to use a non-physiological trick (low ionic strength) to keep the membranes apart, it is conceivable that this separator role is fulfilled by proteins residing in the space between the vesicle and the plasma membrane. Considering that both synaptic vesicles and release sites are indeed crowded with membrane proteins⁴², such a scenario is not unlikely. However, further experiments are needed to determine whether under physiological conditions SNARE nucleation occurs before or after Ca²⁺-triggering in regulated exocytosis of synaptic vesicles.

Methods

Proteins were purified as described^{5,24,25}. Liposomes were prepared by size-exclusion chromatography as described²⁴. Lipid mixing was performed as described²⁴, except that 1.5 mol% 1,1'-dioctadecyl-3,3,3',3'-tetramethylindodicarbocyanine perchlorate (DiD; Invitrogen; emission 670 nm) was used as acceptor fluorophore to reduce cross-talk²⁷. The lipid composition of the R-SNARE liposomes was chosen to mimic the synaptic vesicle⁴² and (unless stated otherwise) consisted of a 5:2:1:1 ratio of PC, phosphatidylethanolamine (PE), PS and cholesterol (all lipids from Avanti Polar Lipids). These liposomes were labeled with 1.5 mol% OG-PE (Invitrogen). The lipid composition of the DiD-labeled Q-SNARE liposomes was identical, except that 1 mol% PC was replaced with the plasma membrane lipid Pi(4,5)P₂. Unless stated otherwise, membrane fusion was triggered with 1 mM Ca²⁺. Ca²⁺ concentrations were calibrated with Fluo-5N and Mag-Fura-2 (Invitrogen). If not stated otherwise, all experiments at high ionic strength were performed in 20 mM K-Hepes pH 7.4, 150 mM KCl. For low ionic strength, the same buffer was used, but now with 5 mM

KCl and 300 mM sucrose. In all cases, lipid mixing could be well inhibited by competitive inhibition with either 10 μ M synaptobrevin-2₁₋₉₆ or with a combination of 10 μ M SNAP-25 and 10 μ M syntaxin-1A₁₈₃₋₂₆₃²⁴.

Protocols have been described for the synaptic vesicles from rat brain³⁷, calcein dequenching²⁴, complex formation by FRET³⁵ and fluorescence anisotropy³⁴. In all cases, protein labeling efficiencies were > 80% as assessed by UV-vis spectroscopy²⁴, except for syntaxin-1A₁₈₃₋₂₆₂ S225C which was only ~30%. EM was performed as described²⁴, except that an additional wash step with 0.1% (w/v) glutaraldehyde in water was performed to remove the sucrose. For the flow cytometry, microfluidic devices were produced using standard polydimethylsiloxane (PDMS) soft lithography^{41,59}. Flow was regulated with home-built, computer controlled pumps. The emission at 540 and 610 nm was recorded simultaneously on a two-camera inverted fluorescence microscope setup. GUVs were prepared by the rehydration of lyophilized small liposomes⁶⁰. Microscale capillary thermophoresis was measured with a NanoTemper NT.015 and 4 nM of liposomes containing 5 mol% OG-PE and 40 nM of DiD-labeled liposomes. DLS was measured on a DynaPro (Wyatt Technology) with a total liposome concentration of 4 nM in case of full-length synaptotagmin-1 or 2 nM liposomes in combination with 10 nM of the soluble C2AB fragment. For the FRET docking experiments (Fig. 4f–g)⁴⁶ the DiI (1,1'-dioctadecyl-3,3,3',3'-tetramethylindocarbocyanine perchlorate; Invitrogen; 1.5 mol%; donor fluorophore) population of liposomes contained 1:4,000 synaptotagmin-1 and the DiD (1.5 mol%; acceptor fluorophore) liposome population contained 1% Pi(4,5)P₂.

For the molecular dynamics simulations, the MARTINI coarse grained forcefield^{48,49} was applied to model synaptotagmin-1 based on the crystal structure⁵⁰. The simulation box of 7.3×6.2×15.0 nm contained a single C2AB protein and 5,376 solvent particles. We performed simulations up to 3 μ s at 310 K while pulling pair-wise with a constant velocity of 10⁻⁵ nm ps⁻¹ on the N-terminus (residue 157), the polybasic lysine patch (234–237) and the two Ca²⁺-binding sites of the C2A- (172, 178, 230, 232 and 238) and C2B-domains (303, 309, 363, 365 and 371). We fixed the structure of the C2A- and C2B-domains with an elastic network that connected each site between 0.5 to 0.9 nm by an harmonic bond with a force constant of 500 kJ mol⁻¹ nm⁻². The center of mass of the binding sites was used to calculate the distances. Distances were calculated shortly before overstretching of the linker, which was apparent from a strong and continuous increase in the bond energy.

Supplementary Material

Refer to Web version on PubMed Central for supplementary material.

Acknowledgments

We thank Alexander Stein and Ursel Ries for protein purification and comments. G.v.d.B is financed by the Human Frontier Science Program. This work was supported by the US National Institutes of Health (P01 GM072694, to R.J.) and the Deutsche Forschungsgemeinschaft SFB755 (to S.T. and S.H.) and SFB803 (to K.M., J.H.R., M.H., U.D., H.G. and R.J.).

References

1. Brunger AT, Weninger K, Bowen M, Chu S. Single-molecule studies of the neuronal SNARE fusion machinery. *Annu. Rev. Biochem.* 2009; 78:903–928. [PubMed: 19489736]
2. Jahn R, Scheller RH. SNAREs—engines for membrane fusion. *Nat. Rev. Mol. Cell Biol.* 2006; 7:631–643. [PubMed: 16912714]
3. Chapman ER. How does synaptotagmin trigger neurotransmitter release? *Annu. Rev. Biochem.* 2008; 77:615–641. [PubMed: 18275379]
4. Martens S, McMahon HT. Mechanisms of membrane fusion: disparate players and common principles. *Nat. Rev. Mol. Cell Biol.* 2008; 9:543–456. [PubMed: 18496517]
5. Radhakrishnan A, Stein A, Jahn R, Fasshauer D. The Ca^{2+} affinity of synaptotagmin I is markedly increased by a specific interaction of its C2B domain with phosphatidylinositol 4,5-bisphosphate. *J. Biol. Chem.* 2009; 284:25749–25760. [PubMed: 19632983]
6. Fernandez I, et al. Three-dimensional structure of the synaptotagmin I C2B-domain: synaptotagmin I as a phospholipid binding machine. *Neuron.* 2001; 32:1057–1069. [PubMed: 11754837]
7. Li L, et al. Phosphatidylinositol phosphates as co-activators of Ca^{2+} binding to C2 domains of synaptotagmin I. *J. Biol. Chem.* 2006; 281:15845–15852. [PubMed: 16595652]
8. Bai J, Tucker WC, Chapman ER. PIP2 increases the speed of response of synaptotagmin and steers its membrane-penetration activity toward the plasma membrane. *Nat. Struct. Mol. Biol.* 2004; 11:36–44. [PubMed: 14718921]
9. Araç D, et al. Close membrane-membrane proximity induced by Ca^{2+} -dependent multivalent binding of synaptotagmin-1 to phospholipids. *Nat. Struct. Mol. Biol.* 2006; 13:209–217. [PubMed: 16491093]
10. Gaffaney JD, Dunning FM, Wang Z, Hui E, Chapman ER. Synaptotagmin C2B domain regulates Ca^{2+} -triggered fusion *in vitro*: critical residues revealed by scanning alanine mutagenesis. *J. Biol. Chem.* 2008; 283:31763–31775. [PubMed: 18784080]
11. Bhalla A, Chicka MC, Tucker WC, Chapman ER. Ca^{2+} -synaptotagmin directly regulates t-SNARE function during reconstituted membrane fusion. *Nat. Struct. Mol. Biol.* 2006; 13:323–330. [PubMed: 16565726]
12. Herrick DZ, Sterbling S, Rasch KA, Hinderliter A, Cafiso DS. Position of synaptotagmin I at the membrane interface: cooperative interactions of tandem C2 domains. *Biochemistry.* 2006; 45:9668–9674. [PubMed: 16893168]
13. Hui E, Bai J, Chapman ER. Ca^{2+} -triggered simultaneous membrane penetration of the tandem C2-domains of synaptotagmin I. *Biophys. J.* 2008; 91:1767–1777. [PubMed: 16782782]
14. Schiavo G, Gu QM, Prestwich GD, Söllner TH, Rothman JE. Calcium-dependent switching of the specificity of phosphoinositide binding to synaptotagmin. *Proc. Natl. Acad. Sci. USA.* 1996; 93:13327–13332. [PubMed: 8917590]
15. Martens S, Kozlov MM, McMahon HT. How synaptotagmin promotes membrane fusion. *Science.* 2007; 316:1205–1208. [PubMed: 17478680]
16. Hui E, Johnson CP, Yao J, Dunning FM, Chapman ER. Synaptotagmin-mediated bending of the target membrane is a critical step in Ca^{2+} -regulated fusion. *Cell.* 2009; 138:709–721. [PubMed: 19703397]
17. Bai J, Wang CT, Richards DA, Jackson MB, Chapman ER. Fusion pore dynamics are regulated by synaptotagmin•SNARE interactions. *Neuron.* 2004; 41:929–942. [PubMed: 15046725]
18. Vrljic M, et al. Molecular mechanism of the synaptotagmin-SNARE interaction in Ca^{2+} -triggered vesicle fusion. *Nat. Struct. Mol. Biol.* 2010; 17:325–331. [PubMed: 20173762]
19. Choi UB, et al. Single-molecule FRET-derived model of the synaptotagmin I-SNARE fusion complex. *Nat. Struct. Mol. Biol.* 2010; 17:318–324. [PubMed: 20173763]
20. Schaub JR, Lu X, Doneske B, Shin YK, McNew JA. Hemifusion arrest by complexin is relieved by Ca^{2+} -synaptotagmin I. *Nat. Struct. Mol. Biol.* 2006; 13:748–750. [PubMed: 16845390]
21. Xue M, Ma C, Craig TK, Rosenmund C, Rizo J. The Janus-faced nature of the C(2)B domain fundamental for synaptotagmin-1 function. *Nat. Struct. Mol. Biol.* 2008; 15:1160–1168. [PubMed: 18953334]

22. Tang J, et al. A complexin/synaptotagmin 1 switch controls fast synaptic vesicle exocytosis. *Cell*. 2006; 126:1175–1187. [PubMed: 16990140]
23. Weber T, et al. SNAREpins: minimal machinery for membrane fusion. *Cell*. 1998; 92:759–772. [PubMed: 9529252]
24. Van den Bogaart G, et al. One SNARE complex is sufficient for membrane fusion. *Nat. Struct. Mol. Biol.* 2010; 17:358–364. [PubMed: 20139985]
25. Stein A, Radhakrishnan A, Riedel D, Fasshauer D, Jahn R. Synaptotagmin activates membrane fusion through a Ca^{2+} -dependent trans interaction with phospholipids. *Nat. Struct. Mol. Biol.* 2007; 14:904–911. [PubMed: 17891149]
26. Chicka MC, Hui E, Liu H, Chapman ER. Synaptotagmin arrests the SNARE complex before triggering fast, efficient membrane fusion in response to Ca^{2+} . *Nat. Struct. Mol. Biol.* 2008; 15:827–835. [PubMed: 18622390]
27. Lee HK, et al. Dynamic Ca^{2+} -dependent stimulation of vesicle fusion by membrane-anchored synaptotagmin 1. *Science*. 2010; 328:760–763. [PubMed: 20448186]
28. Lynch KL, et al. Synaptotagmin C2A loop 2 mediates Ca^{2+} -dependent SNARE interactions essential for Ca^{2+} -triggered vesicle exocytosis. *Mol. Biol. Cell*. 2007; 18:4957–4968. [PubMed: 17914059]
29. Tucker WC, Weber T, Chapman ER. Reconstitution of Ca^{2+} -regulated membrane fusion by synaptotagmin and SNAREs. *Science*. 2004; 304:435–438. [PubMed: 15044754]
30. Rhee JS, et al. Augmenting neurotransmitter release by enhancing the apparent Ca^{2+} affinity of synaptotagmin 1. *Proc. Natl. Acad. Sci. USA*. 2005; 102:18664–18669. [PubMed: 16352718]
31. Margittai M, Fasshauer D, Pabst S, Jahn R, Langen R. Homo- and heterooligomeric SNARE complexes studied by site-directed spin labeling. *J. Biol. Chem.* 2001; 276:13169–13177. [PubMed: 11278719]
32. Fasshauer D, Margittai M. A transient N-terminal interaction of SNAP-25 and syntaxin nucleates SNARE assembly. *J. Biol. Chem.* 2004; 279:7613–7621. [PubMed: 14665625]
33. Parlati F, et al. Rapid and efficient fusion of phospholipid vesicles by the alpha-helical core of a SNARE complex in the absence of an N-terminal regulatory domain. *Proc. Natl. Acad. Sci. USA*. 1999; 96:12565–12570. [PubMed: 10535962]
34. Pobbati AV, Stein A, Fasshauer D. N- to C-terminal SNARE complex assembly promotes rapid membrane fusion. *Science*. 2006; 313:673–676. [PubMed: 16888141]
35. Siddiqui TJ, et al. Determinants of synaptobrevin regulation in membranes. *Mol. Biol. Cell*. 2007; 18:2037–2046. [PubMed: 17360966]
36. Li F, et al. Energetics and dynamics of SNAREpin folding across lipid bilayers. *Nat. Struct. Mol. Biol.* 2007; 14:890–896. [PubMed: 17906638]
37. Holt M, Riedel D, Stein A, Schuette C, Jahn R. Synaptic vesicles are constitutively active fusion machines that function independently of Ca^{2+} . *Curr. Biol.* 2008; 18:715–722. [PubMed: 18485705]
38. James DJ, Khodthong C, Kowalchuk JA, Martin TF. Phosphatidylinositol 4,5-bisphosphate regulates SNARE-dependent membrane fusion. *J. Cell Biol.* 2008; 182:355–366. [PubMed: 18644890]
39. Van den Bogaart G, Hermans N, Krasnikov V, de Vries AH, Poolman B. On the decrease in lateral mobility of phospholipids by sugars. *Biophys. J.* 2007; 92:1598–1605. [PubMed: 17142271]
40. Cerjan C, Barnett RE. The viscosity dependence of a putative diffusion-limited reaction. *J. Phys. Chem.* 1971; 76:1192–1195.
41. Knight JB, Vishwanath A, Brody JP, Austin RH. Hydrodynamic focusing on a silicon chip: mixing nanoliters in microseconds. *Phys. Rev. Lett.* 1998; 80:3863–3866.
42. Takamori S, et al. Molecular anatomy of a trafficking organelle. *Cell*. 2006; 127:831–846. [PubMed: 17110340]
43. Nishiki T, Augustine GJ. Dual roles of the C2B domain of synaptotagmin I in synchronizing Ca^{2+} -dependent neurotransmitter release. *J. Neurosci.* 2004; 24:8542–8550. [PubMed: 15456828]
44. Wienken CJ, Baaske P, Rothbauer U, Braun D, Duhr S. Protein-binding assays in biological liquids using microscale thermophoresis. *Nat. Commun.* 2010; 1:100. [PubMed: 20981028]

45. Duhr S, Braun D. Why do molecules move along a temperature gradient? *Proc. Natl. Acad. Sci. USA*. 2006; 103:19678–19682. [PubMed: 17164337]
46. Yoon TY, Okumus B, Zhang F, Shin YK, Ha T. Multiple intermediates in SNARE-induced membrane fusion. *Proc. Natl. Acad. Sci. USA*. 2006; 103:19731–19736. [PubMed: 17167056]
47. Borden CR, Stevens CF, Sullivan JM, Zhu Y. Synaptotagmin mutants Y311N and K326/327A alter the calcium dependence of neurotransmission. *Mol. Cell. Neurosci*. 2005; 29:462–470. [PubMed: 15886015]
48. Marrink SJ, Risselada HJ, Yefimov S, Tieleman DP, de Vries AH. The MARTINI force field: coarse grained model for biomolecular simulations. *J. Phys. Chem. B*. 2007; 111:7812–7824. [PubMed: 17569554]
49. Monticelli L, et al. The MARTINI coarse grained forcefield: extension to proteins. *J. Chem. Theory Comput*. 2008; 4:819–834. [PubMed: 26621095]
50. Sutton RB, Ernst JA, Brunger AT. Crystal structure of the cytosolic C2A-C2B domains of synaptotagmin III. Implications for Ca^{2+} -independent snare complex interaction. *J. Cell Biol*. 1999; 147:589–598. [PubMed: 10545502]
51. Hu K, et al. Vesicular restriction of synaptobrevin suggests a role for calcium in membrane fusion. *Nature*. 2002; 415:646–650. [PubMed: 11832947]
52. de Wit H, et al. Synaptotagmin-1 docks secretory vesicles to syntaxin-1/SNAP-25 acceptor complexes. *Cell*. 2009; 138:935–946. [PubMed: 19716167]
53. Walter AM, Wiederhold K, Bruns D, Fasshauer D, Sørensen JB. Synaptobrevin N-terminally bound syntaxin-SNAP-25 defines the primed vesicle state in regulated exocytosis. *J. Cell Biol*. 2010; 3:401–413. [PubMed: 20142423]
54. Borisovska M, et al. v-SNAREs control exocytosis of vesicles from priming to fusion. *EMBO J*. 2005; 24:2114–2126. [PubMed: 15920476]
55. Gerber SH, et al. Conformational switch of syntaxin-1 controls synaptic vesicle fusion. *Science*. 2008; 321:1507–1510. [PubMed: 18703708]
56. Schiavo G, Stenbeck G, Rothman JE, Söllner TH. Binding of the synaptic vesicle v-SNARE, synaptotagmin, to the plasma membrane t-SNARE, SNAP-25, can explain docked vesicles at neurotoxin-treated synapses. *Proc. Natl. Acad. Sci. USA*. 1997; 3:997–1001. [PubMed: 9023371]
57. Mohrmann R, de Wit H, Verhage M, Neher E, Sørensen JB. Fast vesicle fusion in living cells requires at least three SNARE complexes. *Science*. 2010; 6003:502–505. [PubMed: 20847232]
58. Ernst JA, Brunger AT. High resolution structure, stability, and synaptotagmin binding of a truncated neuronal SNARE complex. *J. Biol. Chem*. 2003; 278:8630–8636. [PubMed: 12496247]
59. Cooper McDonald J, et al. Fabrication of microfluidic systems in poly(dimethylsiloxane). *Electrophoresis*. 1999; 21:27–40.
60. Doeven MK, et al. Distribution, lateral mobility and function of membrane proteins incorporated into giant unilamellar vesicles. *Biophys. J*. 2005; 88:1134–1142. [PubMed: 15574707]

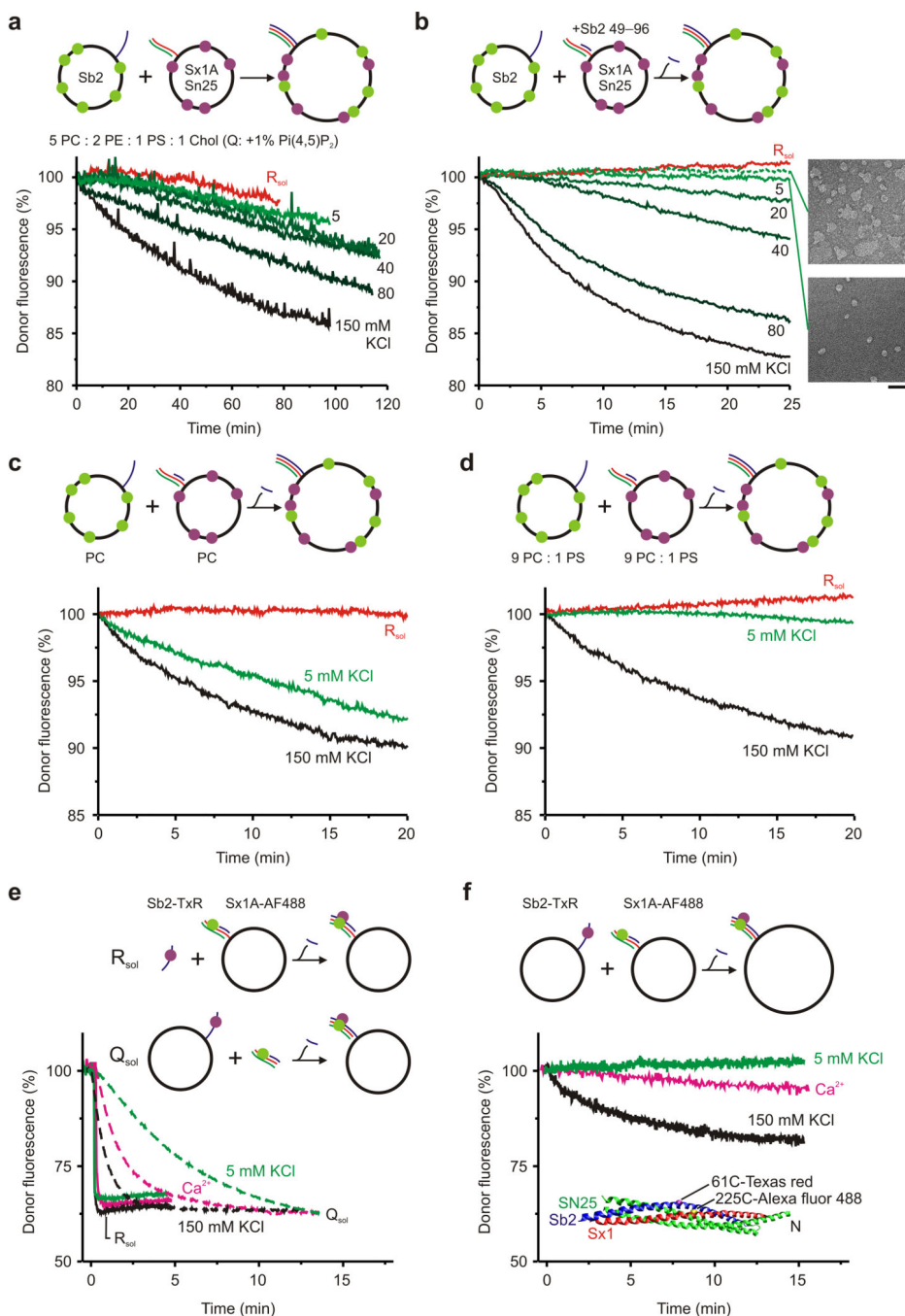


Figure 1. Electrostatic repulsion blocks SNARE-mediated membrane fusion at low ionic strength. **(a)** Lipid mixing of DiD-labeled liposomes containing syntaxin-1A–SNAP-25 with OG-PE-labeled liposomes containing synaptobrevin-2. Membrane fusion results in donor quenching. Fusion was measured at the KCl concentrations indicated. **(b)** As **a**, but now for liposomes containing the synaptobrevin-2_{49–96} stabilized acceptor complex³⁴. The osmolarity was preserved with sucrose. Lipid mixing was still blocked without sucrose (dashed green curve), but the liposomes were deformed by osmotic stress (inset, negative-staining EM;

scale bar, 100 nm). Synaptobrevin-2₁₋₉₆ inhibited fusion (R_{sol} ; for 150 mM KCl). **(c)** As **b**, but now with pure PC liposomes where lipid mixing occurred at both low (green) and normal (black) ionic strength. **(d)** 10% anionic PS blocked fusion at low, but not normal, ionic strength. **(e)** SNARE complex formation by FRET³⁵. The soluble SNARE-domain of synaptobrevin-2 (100 nM; R_{sol} ; solid curves) or syntaxin-1A with SNAP-25 (Q_{sol} ; dashed) resulted in complex formation regardless of ionic strength. **(f)** In contrast, mixing liposomes containing membrane-anchored synaptobrevin-2 and syntaxin-1A resulted in complex formation only at normal but not at low ionic strength regardless of 1 mM Ca^{2+} (pink). The structure⁵⁸ shows the dye positions. The FRET efficiencies are underestimated because the ~20% crosstalk is not accounted for. Typical curves of several repeats are shown. Experiments were performed with 4–8 nM liposomes at 20°C.

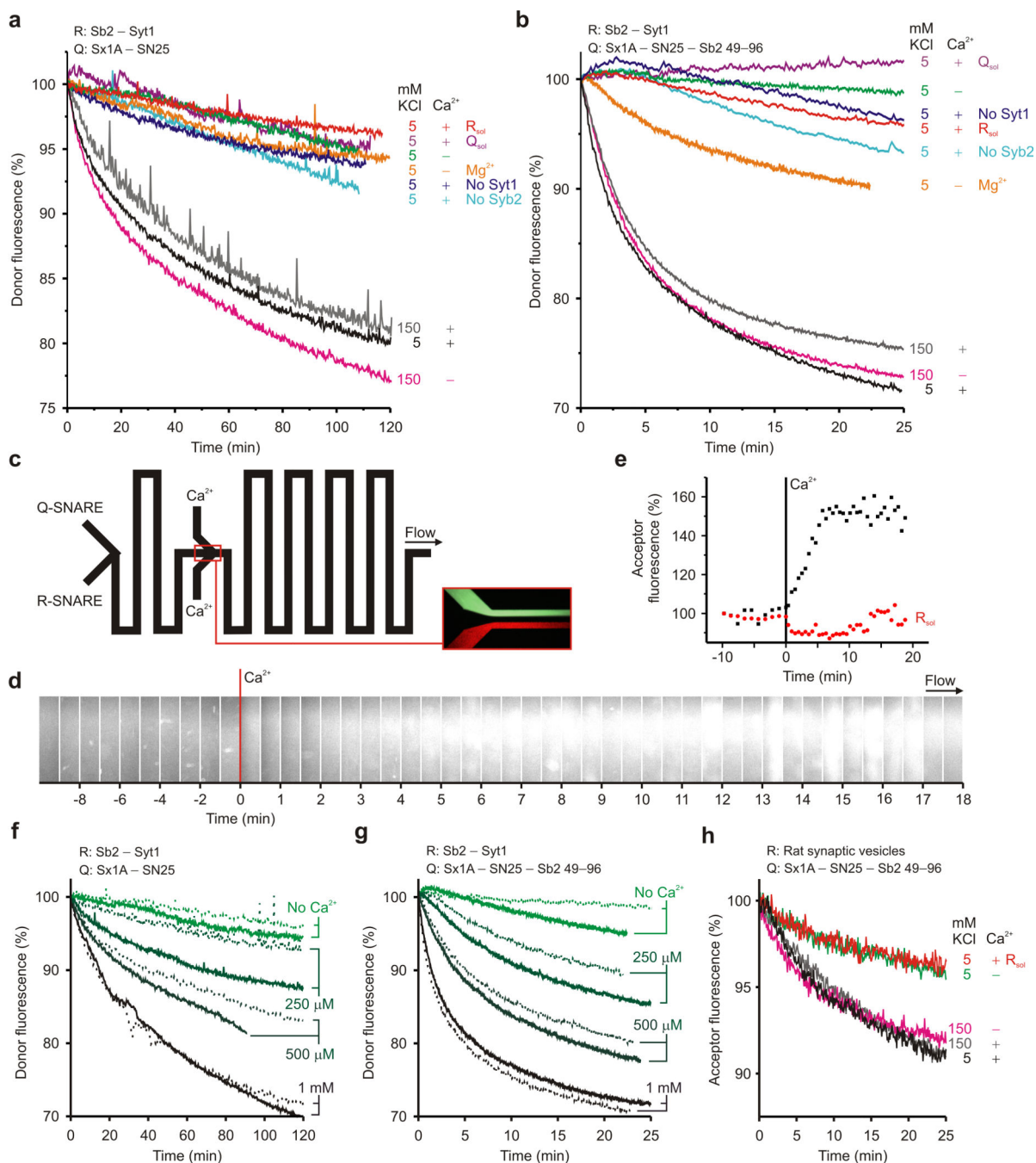


Figure 2.

At low ionic strength, Ca²⁺-synaptotagmin-1 triggers lipid mixing. Lipid mixing of synaptobrevin-2–synaptotagmin-1 liposomes with those containing (a) syntaxin-1A–SNAP-25 and (b) the synaptobrevin-2_{49–96} stabilized acceptor complex³⁴. At low ionic strength, 1 mM Ca²⁺ substantially increased lipid mixing. 1 mM Mg²⁺ resulted in much less fusion. No lipid mixing was observed without synaptotagmin-1 (No Syt1) or synaptobrevin-2 (No Syb2). Synaptobrevin-2_{1–96} (R_{sol}; for 1 mM Ca²⁺) or SNAP-25 and syntaxin-1A_{183–262} (Q_{sol}) inhibited fusion. (c–e) Ca²⁺-triggered lipid mixing by flow

cytometry. **(c)** Donor and acceptor liposomes (as **a**) were mixed in the $23 \text{ cm} \times 100 \text{ }\mu\text{m} \times 80 \text{ }\mu\text{m}$ (LWH) flow chamber. The flow speed was kept constant. At 25% of the channel length, Ca^{2+} was introduced by fast focused mixing. **(d)** Acceptor fluorescence along the channel with fluorescence microscopy and **(e)** binning of the fluorescence. Ca^{2+} specific lipid mixing was observed. **(f)** Lipid mixing at low ionic strength as **a** at the Ca^{2+} concentrations indicated, with (solid) or without (dashed) 0.5 mM Mg^{2+} . **(g)** As **f**, but now with the synaptobrevin-249-96 stabilized acceptor complex. **(h)** Fluorescence dequenching experiment showing Ca^{2+} dependent lipid mixing of synaptobrevin-249-96 stabilized acceptor complex liposomes with purified rat synaptic vesicles³⁷. Experiments were performed with 4 nM liposomes at 20°C . Typical experiments of several repeats are shown.

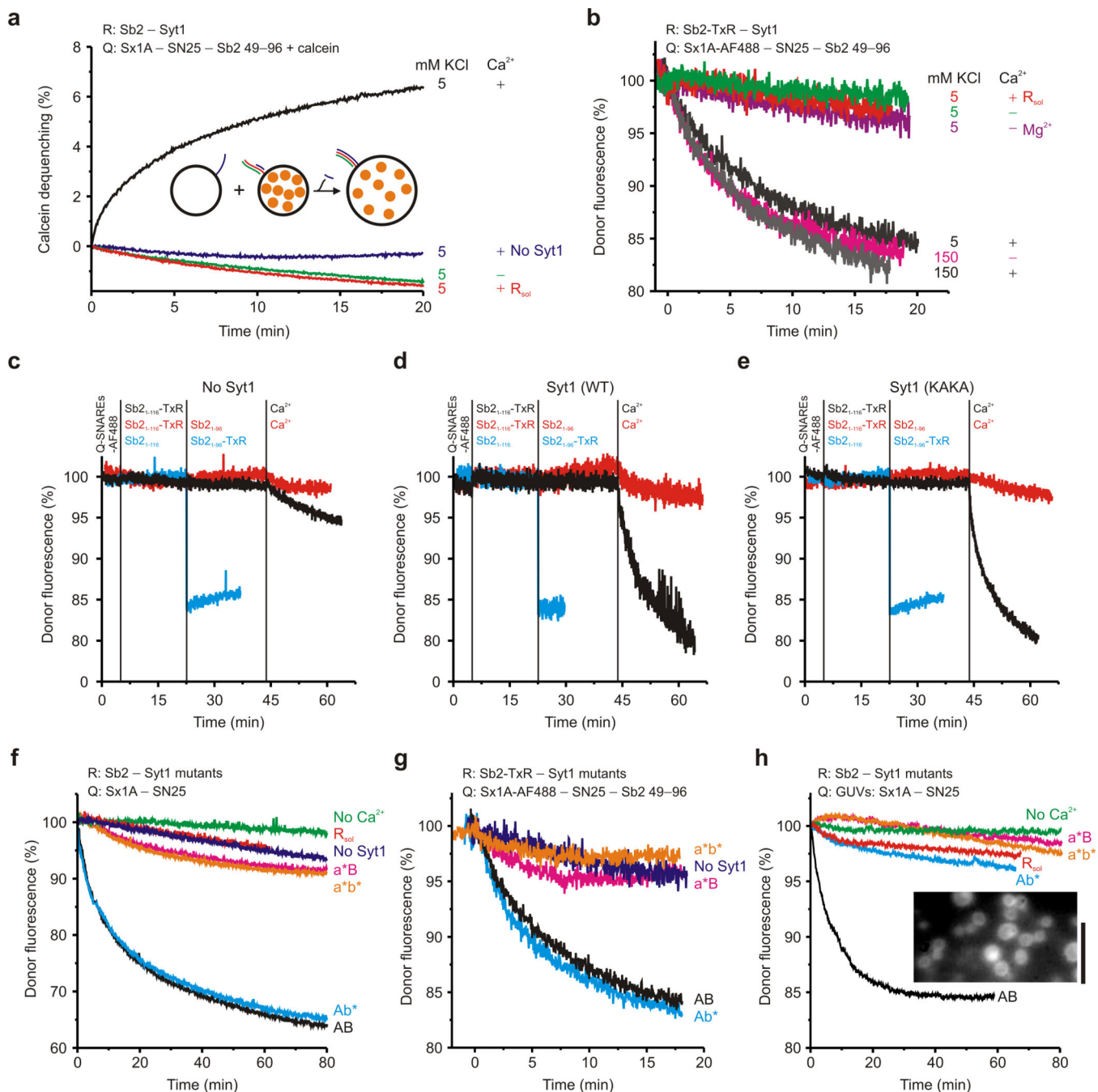
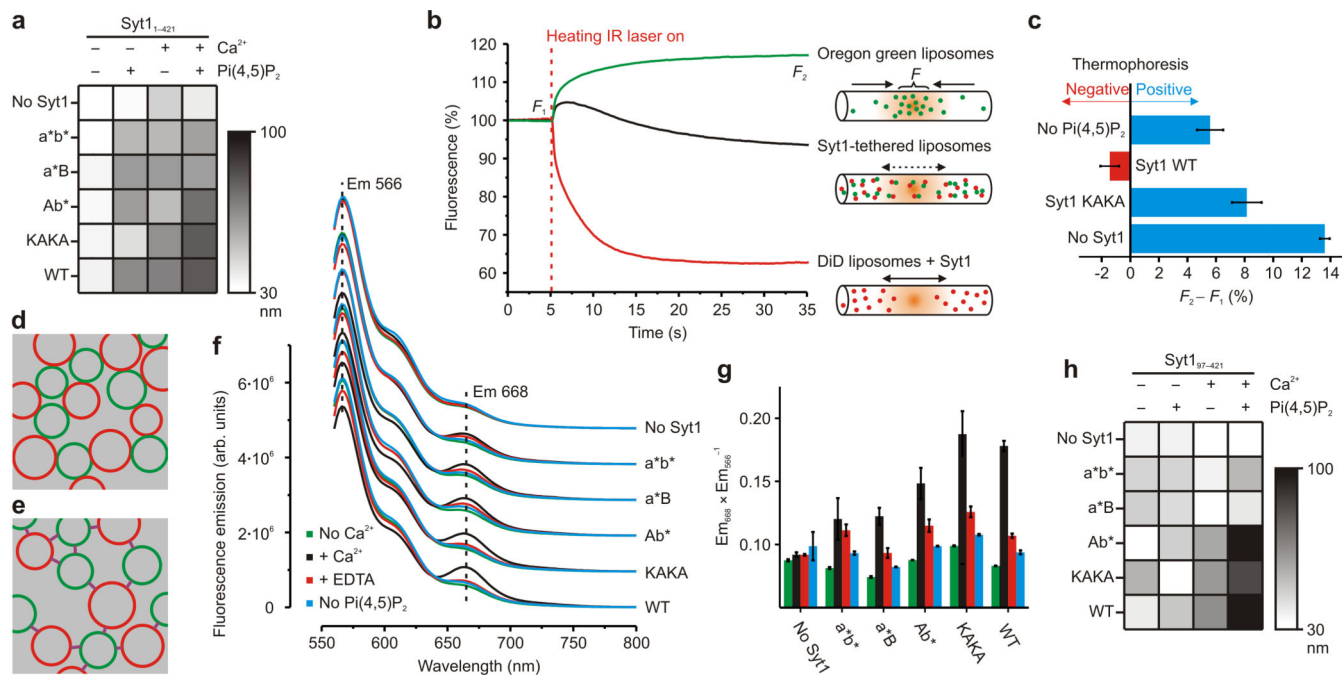


Figure 3. Ca²⁺-synaptotagmin-1 triggers full membrane fusion at low ionic strength. **(a)** Content mixing²⁴ with a self-quenching concentration of calcein encapsulated in liposomes with the stabilized Q-SNARE complex. Fusion with empty R-SNARE liposomes resulted in specific fluorescence dequenching. Synaptobrevin-2₁₋₉₆ (R_{sol}) or absence of Ca²⁺ or synaptotagmin-1 (No Syt1) abolished fusion. **(b)** Ca²⁺-dependent SNARE complex formation by FRET as **1f** with membrane-anchored synaptobrevin-2–synaptotagmin-1. **(c–e)** SNARE complex formation with FRET. Liposomes containing the stabilized Q-SNARE

complex were incubated with synaptobrevin-2₁₋₁₁₆ liposomes without Ca²⁺. The synaptobrevin-2 liposomes contained (c) no, (d) wild-type synaptotagmin-1 or (e) the KAKA mutant. At the indicated times synaptobrevin-2₁₋₉₆ was added, either unlabeled (red curve; in case of Texas-red-labeled synaptobrevin-2₁₋₁₁₆) or Texas-red-labeled (blue; in case of unlabeled synaptobrevin-2₁₋₁₁₆). The black curve shows the control without synaptobrevin-2₁₋₉₆. Membrane fusion was triggered with Ca²⁺. Synaptobrevin-2₁₋₉₆ bound to the Q-SNAREs regardless of the presence of synaptobrevin-2₁₋₁₁₆-synaptotagmin-1 liposomes. (f) Lipid mixing by Ca²⁺-synaptotagmin-1 wild-type (AB) and Ca²⁺-binding disruption mutants to C2B (Ab*), C2A (a*B), or both (a*b*). (g) SNARE complex formation by FRET for the synaptotagmin-1 mutants paralleled lipid mixing. (h) Lipid mixing of synaptobrevin-2-synaptotagmin-1 liposomes with 10–20 μm-sized giant unilamellar vesicles (GUVs) containing the Q-SNAREs (inset, fluorescence microscopy; scale bar, 50 μm). Disrupting Ca²⁺-binding to the C2B-domain abolished fusion with GUVs. ~4 nM liposomes were used at 20°C. Typical curves of several repeats are shown.

**Figure 4.**

Liposome clustering by synaptotagmin-1. **(a)** Dynamic light scattering (DLS) at low ionic strength. Liposomes with 1:4,000 synaptotagmin-1 mutants were mixed 1:1 with $\text{Pi}(4,5)\text{P}_2$ liposomes (No SNAREs; bar-graphs and polydispersities, Supp. Fig. 4c). The grayscale indicates the liposome cluster size. **(b)** Microscale capillary thermophoresis^{44,45} tethering experiment. OG-PE-labeled liposomes move towards the heated spot in a capillary (= negative thermophoresis). In contrast, DiD-labeled liposomes containing synaptotagmin-1 move away from the heated spot (= positive thermophoresis). Tethered liposomes show intermediate thermophoresis. **(c)** The change in OG-PE fluorescence after 30 s heating with the focused IR-laser ($F_2 - F_1$; $n = 3$, \pm s.d.). Tethering was reduced without $\text{Pi}(4,5)\text{P}_2$ or with the KAKA mutant. **(d–e)** Docking arrangements with liposomes tethered at **(d)** close or **(e)** further distance. **(f)** FRET docking⁴⁶ immediately after mixing DiI-liposomes containing 1:4,000 synaptotagmin-1 with DiD-liposomes. No FRET was observed without Ca^{2+} (green), while Ca^{2+} increased FRET (black). 1 mM EDTA (red) showed that this increased FRET was due to close proximity of the membranes. FRET was substantially reduced without $\text{Pi}(4,5)\text{P}_2$ (blue). **(g)** The acceptor over donor fluorescence from **f** (\pm s.d., $n = 3$). **(h)** DLS as **a**, but now with 10 nM of the C2AB fragment (see also Supp. Fig. 4f). Total liposome concentrations were 2–4 nM. Typical data of several experiments are shown.

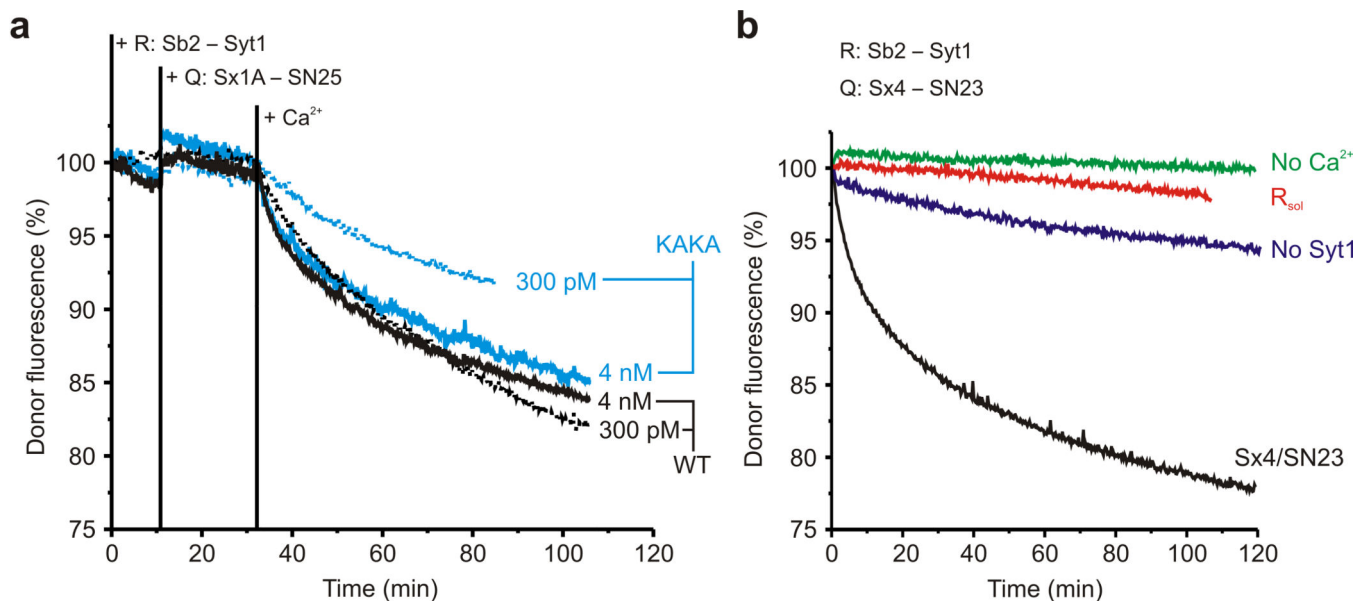


Figure 5.

Preclustering of liposomes accelerates lipid mixing. **(a)** 150 pM or 2 nM of R-SNARE liposomes were preincubated for 20 min with the same amounts of Q-SNARE liposomes. Subsequently, lipid mixing was triggered by addition of Ca²⁺. For the high (4 nM total) liposome concentrations, the lipid mixing efficiency of wild-type synaptotagmin-1 (black curves) was comparable to that of the KAKA mutant (blue curves). In contrast, for the low liposome concentrations (300 pM), the fusion efficiency was substantially reduced for the KAKA mutant compared to wild-type. **(b)** Lipid mixing of full-length synaptotagmin-1–synaptobrevin-2 liposomes with liposomes containing the Q-SNAREs of constitutive exocytosis (syntaxin-4 and SNAP-23). No fusion was observed in absence of Ca²⁺ (No Ca²⁺) and fusion could be blocked with synaptobrevin-2_{1–96} (R_{sol}). All fusion experiments were performed at 20°C. Typical curves of multiple repeats are shown.

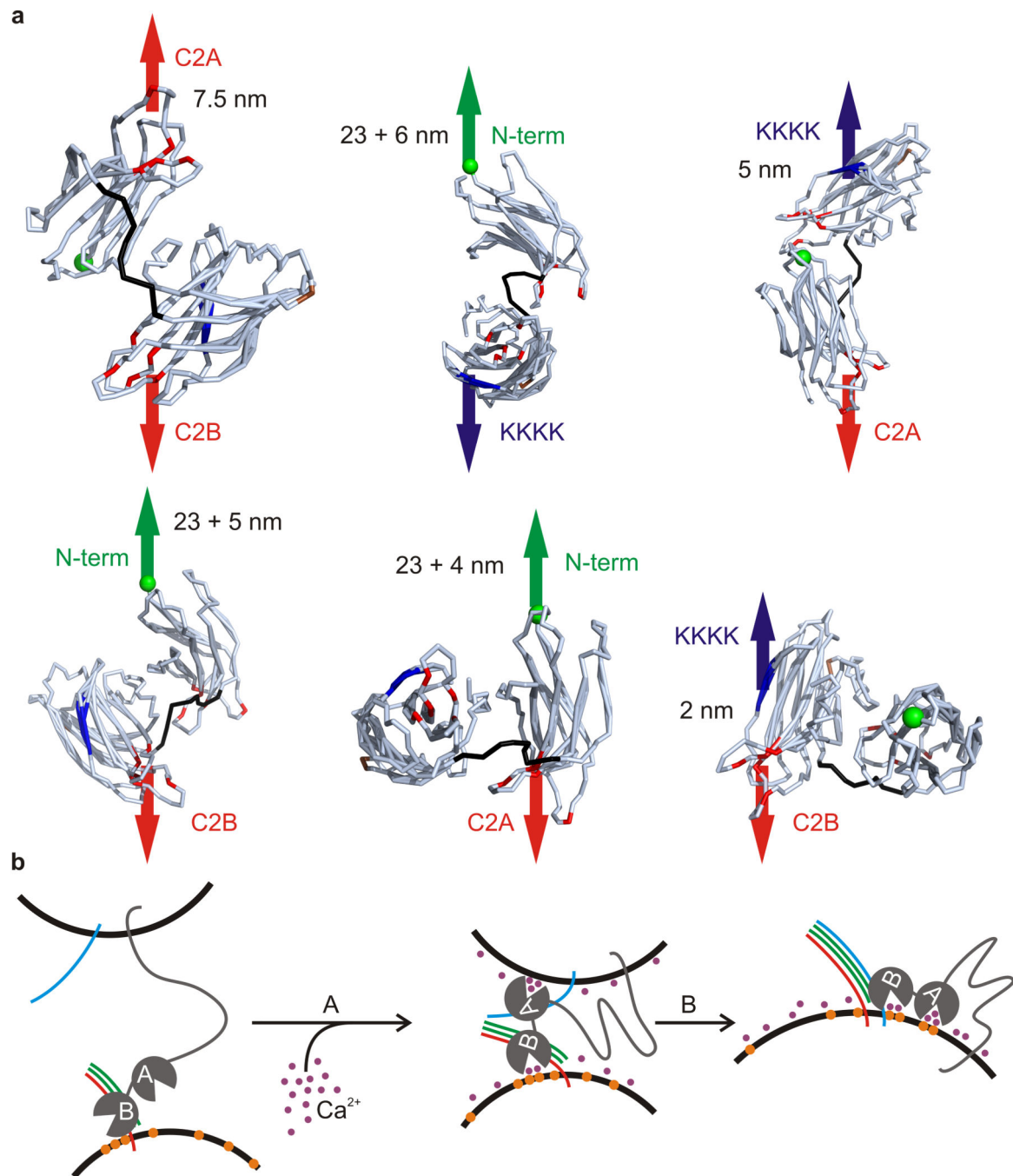


Figure 6.

Models of synaptotagmin-1 distance regulation. **(a)** Molecular dynamic simulations to estimate the maximal distances between the various domains. In the simulations, we pulled pair-wise on various membrane binding sites of the C2AB-domain: the N-terminus (green), the polybasic lysine patch (blue; KKKK) and the Ca^{2+} -binding sites of the C2A- and C2B-domain (red). The two conserved arginines (R398 and R388) are shown in brown; the linker is in black. The N-terminus is connected to the transmembrane helix with a 61 residue linker that can extend to ~ 23 nm. Maximal distances are indicated in the figure; these are an

approximate for the tethering distances of the membranes, but do not take into account additional interactions such as membrane insertion and bending. **(b)** Model for synaptotagmin-1 mediated lipid mixing. In the absence of Ca^{2+} , synaptotagmin-1 (grey) tethers to anionic membranes, and particularly to $\text{Pi}(4,5)\text{P}_2$ (orange) via its polybasic lysine patch. The distance is too far for SNARE formation to occur (synaptobrevin-2: blue; Syntaxin-1A: red; SNAP-25: green). (Step A) In the presence of Ca^{2+} (purple), a transitional conformation change occurs and synaptotagmin-1 binds the membrane via its calcium binding pockets and basic residues on the C2AB-domain⁹. This drives the membranes together and SNARE complex formation can occur. (Step B) The SNARE complex formation drives membrane fusion.

Author Manuscript

Author Manuscript

Author Manuscript

Author Manuscript